# Augmentation of Vegetation Index Curves Considering the Crop-Specific Phenological Characteristics

P. V. Arun, *Student Member, IEEE*, and Arnon Karnieli, *Member, IEEE*

***Abstract*—The state-of-the-art crop phenological classifiers use vegetation index (VI) time-series data and deep learning (DL) techniques. However, the scarcity of training samples limits the performance of these approaches. Unlike the conventional augmentation techniques, the data augmentation of VI curves should preserve the crop-specific phenological events. The DL-based augmentation approaches do not give good results when the training samples are limited. Also, the conventional approaches such as translation, rotation, scaling, and wrapping do not preserve the characteristic features of the index curves, thereby making them inappropriate for the VI-curve-based augmentations. This article proposes a non-DL-based data augmentation strategy that requires only a minimal number of actual training samples. In the proposed approach, the periodic phenological events and the underlying trend for each crop class are modeled to improve the augmentation. The trends of different crop classes are estimated by jointly maximizing the autocorrelation and variance, while the optimal subsequences are generalized as the phenological events. The proposed augmentation strategy of using Maximal overlap discrete wavelet transform for obtaining the surrogates that retain the crop-specific features and periodicities significantly improves the results. It may be noted that the proposed approach does not alter the wavelet coefficients that are characteristics of a given crop class. The experiments using time series VI data, covering 90 fields of wheat, and 60 fields of barley, confirm better accuracy of the proposed augmentation approaches as compared to the prominent approaches.**

***Index Terms*—Crop classification, deep learning, maximal overlap discrete wavelet transform, normalized differential vegetation index (NDVI), time series, VENμS.**

## I. Introduction

EXTRACTION of information from earth observation data forms the basis of many applications in the agriculture domain ranging from acreage estimation, crop condition assessment, and yield forecasting. Recently, multitemporal satellite/airborne data is being explored to model different periodic events in the growth cycle of crops [1]–[6]. Most of the phenology-based classifiers use vegetation index (VI) time-series data [e.g., normalized differential VI (NDVI)], estimated from temporal images over a given season, as phenology fingerprints to model seasonal variations of different crops [1], [7]–[10]. Recent studies indicate that conjunctive consideration of feature extraction and classification by deep learning models, improves the time-series classifiers [11], [12]. However, the lack of sufficient training samples affects the implementation of DL-based approaches for VI-curve-based classification.

Different strategies such as network pruning [13], transfer learning [14]–[17], deep data augmentation [5], [18]–[21], and generative networks [19], [22]–[25] are being widely used to address the scarcity of training samples. The network pruning strategies, which remove the least useful filters and channels, have limited success as the complex datasets still require a lot of training samples [13]. Recently, generative adversarial network (GAN) [26] and its variants have been employed to resolve the bias and class imbalance problem by generating synthetic class-specific samples [26]–[28]. However, generative models trained on a class imbalance dataset may not necessarily capture the actual data distribution, especially in extreme conditions, resulting in artifacts [29]–[33]. Different alternatives of GANs such as auxiliary classifier GAN (AC-GAN) [30], conditional GAN (C-GAN) [27], and few shot classifier GAN (FSCGAN) [31] avoid generating minority classes in extreme class imbalance cases [32], [33]. The samples generated by FSCGAN are affected by artifacts or white noise patches [31]. The multiple fake classes GAN model adopted generator conditioning and resampling of minority classes to generate images from imbalance classes [34]. Most of these GAN-based approaches are suited for the image datasets and are not directly applicable to the multitemporal VI data [35], [36]. Besides, the DL-based augmentation approaches do not generally consider the features and phenological events specific to each crop and require a considerable amount of training samples [31], [35]. The transfer learning-based approaches project the label information to unlabeled data using proximity measures [37]. Most of these techniques still require enough labeled information to capture the intra-class variability. Additionally, their effectiveness is sensitive to the efficiency of the adopted distance measures and the similarity of the source and target distributions [13], [37].

The non-DL-based data augmentation techniques are gaining popularity as they address the sample scarcity by learning the class-specific features from a small set of samples. Details of the commonly employed non-DL-based augmentations discussed in this study can be referred from [38]–[42]. Reclassification and

Manuscript received July 23, 2021; revised November 9, 2021, November 16, 2021, and December 24, 2021; accepted December 26, 2021. Date of publication January 13, 2022; date of current version January 27, 2022. This work was supported by the Israeli French High Council for Scientific & Technological Cooperation, Research Program "Maïmonide-Israel", under Contract 3-15832. *(Corresponding author: Arnon Karnieli.)*

The authors are with the Swiss Institute for Dryland Environmental and Energy Research, Jacob Blaustein Institutes for Desert Research, Ben Gurion University of the Negev, Sede Boker Campus 8499000, Israel (e-mail: arunvi2601@gmail.com; karnieli@bgu.ac.il).

Digital Object Identifier 10.1109/JSTARS.2022.3142395

This work is licensed under a Creative Commons Attribution-NonCommercial-NoDerivatives 4.0 License. For more information, see https://creativecommons.org/licenses/by-nc-nd/4.0/

removal of samples, proposed to improve the quality of training data, do not apply to the generation of training samples [43], [44]. The non-DL-based augmentation techniques generally adopt transformations to generate samples similar to the available ones without using complex models. The conventional approaches, such as geometric transformations, kernel filters (smoothing or enhancement), image mixing (interchanging slices), and random erasing (removing random slices), are suited only for image-related tasks [35], [40], [42]. For time-series data, augmentations such as jittering (random noise addition) [45], slicing (cropping) [46], magnitude warping (smooth elementwise magnitude change) [18], [38], permutation (rearranging slices) [45], [47], rotation (flipping for univariate; rotation for multivariate) [35], scaling (patternwise magnitude change) [47], random warping in the time dimension (time step deformation) [45], [47], and frequency warping (frequency deformation) [48] are adopted. The slicing-based augmentations responded positively with more extended time series, but pattern mixing methods are negatively correlated to the time series length. Most of these approaches result in massively inflated dataset sizes that may cause overfitting in domains with limited data [36]. Moreover, they fail to properly model the characteristic phenological features of the VI curves [35], [46].

The conventional augmentation approaches have little or converse effect on the performance of advanced time-series networks such as long short-term memory (LSTM), bidirectional LSTM, LSTM-fully connected network, and ResNet [35]. Alternatives of dynamic time wrapping (DTW) have been adopted for leveraging the phenological information of labeled samples to generate labels of unlabeled ones [44], [49]–[51]. However, these approaches require finetuning of the proximity parameters and the samples to have less intraclass variability. Recently, Fourier transform (FT) based data augmentation approaches, such as Iterative amplitude adjusted FT (IAAFT), adopted phase alternations to preserve the power- and cross-spectrum of the signals [52]–[54]. The stochastic versions of IAAFT, which implement fractional amplitude adjustment, preserve the amplitude distribution, and the power spectrum of the measured time series [55]. Kayal *et al.* [56] employed jittering of discrete cosine and wavelet transforms' bases to generate surrogates having slightly different noise properties. Maximal overlap discrete wavelet transform (MODWT) based augmentation approaches combine IAAFT schemes to each level of MODWT coefficients without assuming stationarity [57], [58]. Although transform-based approaches do not require many training samples, they fail to model the characteristic phenological events of different crops. Hence, wavelet- and Fourier-based approaches have limited applications for the augmentation of the VI curves.

This article investigates augmentation approaches that consider the characteristic features and phenological events of different crops. This article hypothesizes that augmentations of VI curves should not alter the phenological events and their characteristics. The adopted approaches and optimizations should model the phenological characteristics and consider the existing samples, class imbalances, and intra- and interclass variances. The proposed non-DL-based augmentations are hypothesized to be suitable for addressing the lack of training samples compared to the DL-based approaches. Additionally, the proposed approaches do not require finetuning of the smoothing parameters. Based on the abovementioned discussions, the main contributions of this research can be summarized as follows.

1) Modeling of the phenological events specific to different crops with minimum training samples.
2) Augmentation of index curves preserving the phenological events.
3) Reduction of training sample requirement and computational complexity for effective augmentation

## II. Proposed Approach

Consider a vegetation index curve v**,** constituting VI values derived from N multitemporal images, thus having a vector length N. Let there be C types of crops whose temporal VI curves are considered. This article constructs surrogate VI curves of different crop classes for addressing the scarcity of training samples to improve the classification. The augmentations are implemented in an interpretable latent space considering the characteristic features and phenological events of each crop. In addition, the class imbalance, existing samples, and intra- and interclass variances are also considered. The following sections discuss the strategies adopted to formulate an optimal framework to accomplish the same.

### *A. Extraction of Class-Specific Trend and Phenological Events From Index Curves*

The index curves of a given crop class are decomposed to model the trend and phenological characteristics. The seasonality of a curve denotes periodic patterns that fluctuate near a baseline, and trend describes the baseline [57]. For a given class of crops, the denoised index curve $\mathrm{v}^{\mathrm{c}}$ can be decomposed as

$$v^c = \tau^c + S^c + \gamma^c \tag{1}$$

where $\tau^{\mathrm{c}}$ is the crop-specific baseline curve, c denotes the crop class, $S^{\mathrm{c}}$ the phenological events or the seasonality, and $\gamma^{\mathrm{c}}$ the remainder of the index curves.

The trend $\tau^c$ of a group of p index curves of the $c$th crop class is estimated based on the maximization of autocorrelation as

$$\mathrm{w}' = \underset{\mathrm{w}}{\operatorname{argmax}} \left\{ \rho \left( \mathrm{wV}_{\mathrm{t}}^{\mathrm{c}}, \mathrm{wV}_{\mathrm{t+1}}^{\mathrm{c}} \right) \right\} \tag{2}$$

$$\tau^{\mathrm{k}} = \mathrm{w}' \mathrm{V}_{\mathrm{t}}^{\mathrm{c}} \tag{3}$$

where $\rho(.,.)$ denotes the autocorrelation of the index curves, w the transformation matrix, $\mathrm{w}'$ the maximum autocorrelation factor, $\mathrm{V}_{\mathrm{t}}^{\mathrm{c}}$ and $\mathrm{V}_{\mathrm{t+1}}^{\mathrm{c}}$ the matrices of the index curves and their time-shifted versions, respectively. Based on [59], (3) is reformulated as

$$\tau^{\mathrm{k}} = \left( \mathrm{C}^{\frac{1}{2}} \mathrm{C}_{\delta} \mathrm{C}^{-\frac{1}{2}} \right) \mathrm{V}_{\mathrm{t}}^{\mathrm{c}} \tag{4}$$

where C denotes the covariance matrix of the index curves, $\mathrm{C}_{\delta}$ is the p $\times$ p covariance matrix of the p time-differenced index curves, and $\mathrm{V}_t^c$ the index curve matrix. The trend computation, based on autocorrelation maximization, is invariant to rescaling and recombining the original data [59].

The phenological events of crop classes are modeled upon the subsequences that cause entropy gain to classify the index curves. In this regard, the joint learning of optimal subsequences and hyperplane is formulated as

$$\underset{\mathrm{S,\ W}}{\operatorname{argmin}} \mathrm{L}\left(\mathrm{y_i}, \tilde{\mathrm{y}}_\mathrm{i}\right) + \lambda_\mathrm{W} \left\|\mathrm{W}\right\| \tag{5}$$

where L(.) denotes the misclassification loss, ||.|| the L2 norm, $\lambda_\mathrm{W}$ is the scaling constant, and $\mathrm{y_i}$ and $\tilde{y}_i$, respectively, the expected and predicted labels. It may be noted that learning of the subsequences s is incorporated in as the following:

$$\widetilde{\mathrm{y}}_\mathrm{i} = \mathrm{W}_0 + \sum_{\mathrm{k}=1}^{\mathrm{K}} \mathrm{M_{i,k}W_k},\ \forall \mathrm{i} \in \{1,\ \ldots,\ \mathrm{p}\} \tag{6}$$

where $\mathrm{W}_0$ is the bias, W is the model weights, M is the predictors in the transformed space, p is the number of index curves, and K is the number of subsequences. Adopting a differentiable proximal approximation, as discussed in [60], the predictor M is modeled as

$$\mathrm{M_{i,k}} = \frac{\sum_{\mathrm{j}=1}^{\mathrm{J}} \mathrm{D_{i,k,j}}\ \mathrm{e}^{\alpha \mathrm{D_{i,k,j}}}}{\sum_{\mathrm{j'}=1}^{\mathrm{J}} \mathrm{e}^{\alpha \mathrm{D_{i,k,j'}}}} \tag{7}$$

where $\alpha$ denotes the tunable parameter and $\mathrm{D_{i,k,j}}$ the distance between the *j*th segment of series i and the *k*th subsequence. The distance between the *i*th index curve $\mathrm{v_i^c}$ and the *k*th subsequence $\mathrm{S_k^c}$ is defined as

$$\mathrm{D_{i,k,j}} = \frac{1}{\mathrm{N}} \sum_{\mathrm{l}\,=\,1}^{\mathrm{N}} \left(\mathrm{v_{i,j+l-1}^c} - \mathrm{S_{k,l}^c}\right)^2 \tag{8}$$

where $\mathrm{v_i^c}$ denotes the *i*th index curve of the *c*th crop class, $\mathrm{S_k^c}$ denotes the *k*th subsequence of the *c*th crop class, and N is the total number of classes. It may be noted that instead of using the subsequences, only the most relevant ones are chosen. In this context, the most likely input $\omega_\mathrm{c}$ for the *c*th crop class is found by optimizing

$$\omega_\mathrm{c} = \max_{\mathrm{v}} \left(\log \mathrm{p(c|v)} + \log \mathrm{p\,(v)}\right) \tag{9}$$

where $\mathrm{p(c|v)}$ and $\mathrm{p(v)}$ are the class conditioned data density and data model, respectively. The importance of a subsequence is measured by estimating its distance from the segments of the representative curves through DTW based distance measure [49].

### *B. Wavelet Transform-Based Augmentation of the Index Curves Preserving the Characteristic Features of Different Crops*

The Maximal overlap discrete wavelet transform (MODWT) [61] decomposes the original signal based on the quadrature mirror filter that divides the frequency band. The discrete wavelet transform reduces the number of signal samples in each decomposition level while MODWT maintains the signal length. The VI curve v can be decomposed based on MODWT as

$$\mathrm{v_t} = \tilde{\mathrm{S}}_{\mathrm{J,t}} + \sum_{\mathrm{j}=1}^{\mathrm{J}} \tilde{\mathrm{D}}_{\mathrm{j,t}},\ t = 1, \ldots,\ N \tag{10}$$

where J is the number of scales, N is the length of the index curve, and $\widetilde{\mathrm{S_J}}$ and $\widetilde{\mathrm{D_j}}$, respectively, denote the tendency and local details of the index curve v at each scale. The proposed augmentation strategy adopts a stochastic version of IAAFT algorithm [54], [55] to each set of the detailed coefficients independently to obtain randomized values that retain the original values and periodicities. It should be mentioned that both the amplitude spectrum and phase spectrum are perturbed at each level of MODWT coefficients. The approach does not alter the wavelet coefficients that are characteristics of a given crop class. These distinctive wavelet coefficients are determined based on the trends and prominent subsequences of the corresponding crop classes. In addition, a threshold based on the unaltered fractional energy of the curves is also employed. As the wavelet power spectrum is proportional to the coefficients, the threshold $\tau$ for unaltered energy of the given index curve is formulated as

$$\tau = 1 - \frac{\sum_{i\,=\,1}^{N} \sum_{j\,=\,1}^{J} D_{ij}^2}{\sum_{i\,=\,1}^{N} \sum_{j\,=\,1}^{J} \tilde{D}_{ij}^2} \tag{11}$$

where N is the length of the index curve, J is the number of scales, and D and $\tilde{\mathrm{D}}$, respectively, denote the unaltered and altered wavelet coefficients.

### *C. DL Model for Phenological Classification of Crops*

Prominent DL-based classification models applicable to the VI curves are employed for analyzing the effectiveness of the proposed augmentation scheme. LSTM based approaches consider the current and previous VI values using a gated network to assign the crop labels. This article adopts a 27-layer stacked LSTM architecture similar to the discussions in [62]. The approach uses the time-frequency and time-space properties of the index curve as a robust tool for modeling the index curves. The GAN-based VI curve classification approach, adopted in this article, jointly optimizes the supervised and adversarial losses to learn an embedding space to preserve the temporal dynamics. As discussed in [78], the framework employs a one-dimensional convolutional GAN having a depth of 38 layers.

### *D. Evaluation of the Data Augmentation Techniques*

The characteristic phenological events, such as the planting, heading, and harvesting, are specific to a given crop. These events are reflected in the VI values and can be estimated from the index curves. Comparing the phenological events estimated from the surrogate and actual index curve samples serves as an evaluation measure for the data augmentation. In addition, a comparison of the trend of the available index curves with those of the surrogates can also be used as an evaluation measure. Large deviations of the surrogates and their trends respectively from the characteristic phenological events (measured in terms of days) and trends (measured in terms of cosine dissimilarity measure) indicate the ineffectiveness of the augmentation strategy.

The DL-based classification models (see Section II-C) are also employed to evaluate the effectiveness of the augmentation techniques. High values of the confusion-matrix-based accuracy

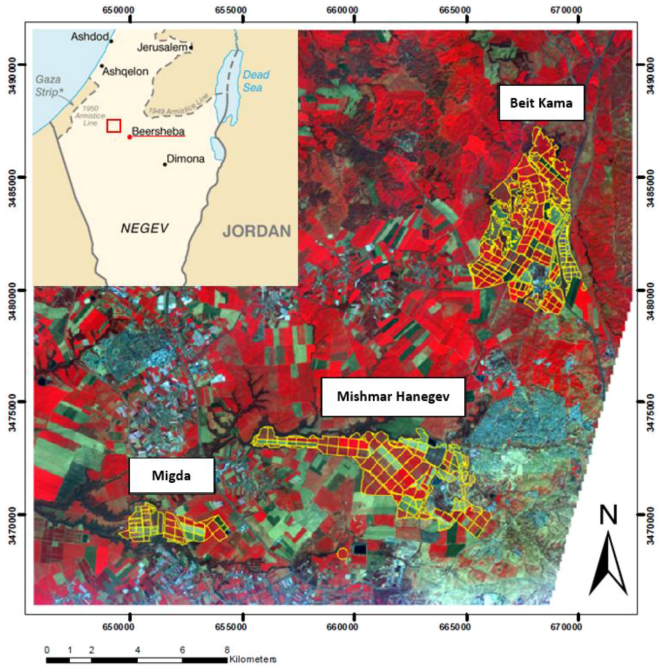


Fig. 1. Location map of the study fields in Israel over a VENμS false color composite image.

measures such as overall accuracy and Kappa statistics indicate that the training samples are well augmented, preserving the crop-specific phenological characteristics.

## III. Experiments

For analyzing the proposed augmentation approach concerning the VI curve classification, multitemporal VEN$\mu$S images covering 90 fields of wheat and 60 fields of barley are employed. The study area is shown in Fig. 1. The VEN$\mu$S sensor (https://karnieli-rsl.com/ven$\mu$s) is characterized by a high spatial resolution of 5 m, a high spectral resolution of 12 narrow bands in the visible to near-infrared regions of the spectrum, and a high revisit time of 2 days at the same viewing and azimuth angles. The NDVI of fields computed over three crop years, 2018, 2019, and 2020 are used for the analysis. It should be mentioned that the VI curves, having a vector length of 27, are used for training the classification models. The shapefiles of crop fields and the cropping, harvesting, and irrigation information obtained from framers serve as ancillary data for labeling the phenological curves. In the experiments adopted in this article, 400 actual (among available 900) and 1600 augmented samples are employed for training the model. It is to be noted that 60–100 samples in proximity are employed to generate an augmented sample to consider the spatial autocorrelation. For all the experiments, a grid search-based approach was adopted to finetune the values of $\alpha$ and $\lambda_W$ (see Section II-A) that are empirically set to 0.89 and 0.40, respectively. Among 900 actual samples, 400 are used for training, 200 for validation, and 300 for testing.

The classification models, adopted in this article to evaluate the augmentation approaches, are trained for a mini-batch size of 200; momentum and weight decay for the backpropagations are set to 0.8 and $10^{-3}$, respectively (obtained through cross validation); learning rate is initially set to 0.6 and is depreciated by a factor of 10 after every 100 epochs. All the models are analyzed for 200 epochs.

TABLE I
Comparison of the Augmented Samples With the Actual Samples for Wheat and Barley Crop

| Data Augmentation Technique | Cosine similarity of augmented and actual samples for wheat | Cosine similarity of augmented and actual samples for barley |
|---|---|---|
| Fourier based [54] | 0.958 | 0.941 |
| Wavelet transform based [53] | 0.964 | 0.949 |
| The proposed approach without modelling the trends and phenological | 0.978 | 0.972 |
| events as discussed in section 2A | | |
| DL based [18] | 0.967 | 0.961 |
| Proposed approach | 0.998 | 0.994 |

### A. Phenological Characteristics of the Surrogates

In order to compare the effectiveness of the augmentation schemes, a cosine-similarity-based comparison of the augmented samples with the actual samples for each of the approaches is presented in Table I. As is evident, the proposed augmentation approach gives the maximum average cosine similarity indicating a better augmentation. However, to further evaluate the effectiveness of augmentation, a comparison based on the phenological characteristics is preferred.

The change in greenness estimated using VI over a period is the characteristics of a given crop type. Hence, this article analyzes the changes in VI, corresponding to planting, heading, and harvesting events, to estimate the correctness of the augmented index curves. The VI of fields decreases during the planting period and increases again after planting. The maximum VI appears around the heading phase and decreases abruptly because of harvesting. In this regard, the heading date is estimated as the duration with the maximum VI in the time profile of the phenological curves. The date of an inflection point later than a fixed number of days (specific to the crop understudy) after the estimated heading date is defined as the harvesting date. The minimal and inflection points earlier than a fixed number of days (specific to the crop understudy) from the estimated heading date are identified as the planting date. An illustration of the augmented samples for barley crops, presented in Fig. 2, shows the variation of NDVI ($x$-axis) with respect to the no. of times the samples have been collected ($y$-axis). It may be noted that the NDVI samples were computed six times in a given month. Fig. 2 illustrates features preserved and the variabilities introduced. It may be noted that the crop-specific events have been well preserved, i.e., the sowing, heading, and harvesting periods of the augmented samples are consistent with the metadata obtained from the farmers.

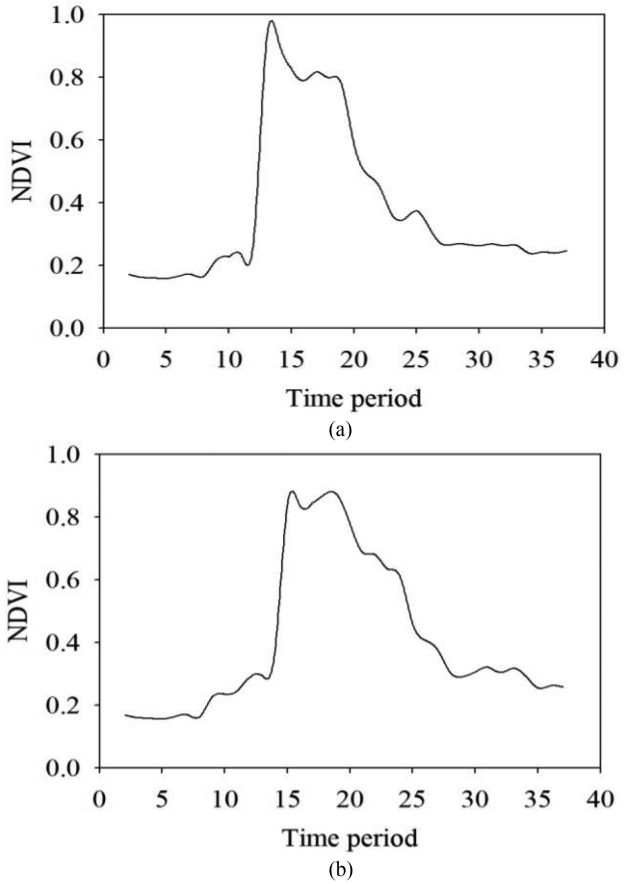


Fig. 2. Two VENμS-derived augmented samples for barley crops: (a) sample-1 and (b) sample-2.

Tables II and III show the performance of the different augmentation methods in preserving the distinct phenological events of the wheat and barley crops. As is evident, Fourier- and wavelet-based augmentations alter the crop-specific characteristic features of the index curves. The proposed approach gives accurate results owing to the consideration of the crop-specific phenological characteristics. It is shown that the planting, heading, and harvesting periods are very accurately preserved in the surrogate samples generated through the proposed approach. In addition, as is evident from Table IV, the trend of each crop class also aligns well with the trend of the corresponding surrogate samples. The plot depicting actual and estimated NDVI during different phenological events is presented in Fig. 3. It may be noted that the y-axis (Time period) denotes the sampling time period in which the temporal images were collected (36 times in 6 months). The comparative analysis presented in Table V indicates that the proposed approach performs well compared to the other approaches in terms of computational efficiency. It may be noted that the root-mean-square error (RMSE) for the growing period of the proposed approach is less than that of other phenological dates. This can be attributed to the fact that growing period covers a lengthier duration as compared to the other phenological events making it easier for the approach to select and generalize the most relevant features.

TABLE II
COMPARISON OF RMSE OF THE ESTIMATED PHENOLOGICAL DATE AND GROWING PERIOD AGAINST THE STATISTICAL DATA FOR THE WHEAT CROP

| Data Augmentation Technique | RMSE for the growing period (no. of days) | RMSE for the planting date (no. of days) | RMSE for the heading date (no. of days) | RMSE for the harvesting date (no. of days) |
|---|---|---|---|---|
| Fourier based [54] | 12.30 | 14.30 | 16.73 | 8.4 |
| Wavelet transform based [53] | 9.70 | 8.90 | 10.60 | 9.25 |
| The proposed approach without modelling the trends and phenological events as discussed in section 2A | 5.8 | 3.3 | 3.5 | 5.4 |
| DL based [18] | 11.20 | 10.40 | 8.39 | 10.04 |
| Proposed approach | 1.72 | 2.54 | 1.62 | 3.84 |

TABLE III
COMPARISON OF RMSE OF THE ESTIMATED PHENOLOGICAL DATE AND GROWING PERIOD AGAINST THE STATISTICAL DATA FOR BARLEY CROP

| Data Augmentation Technique | RMSE for the growing period (no. of days) | RMSE for the planting date (no. of days) | RMSE for the heading date (no. of days) | RMSE for the harvest date (no. of days) |
|---|---|---|---|---|
| Fourier based [54] | 17.28 | 10.07 | 15.35 | 12.96 |
| Wavelet transform based [53] | 14.17 | 16.89 | 14.28 | 10.03 |
| Proposed approach without modelling the trends and phenological events as discussed in section 2A | 4.06 | 2.48 | 4.90 | 1.76 |
| DL based [18] | 17.69 | 12.28 | 15.28 | 14.45 |
| Proposed approach | 1.53 | 1.89 | 1.64 | 2.81 |

### B. Improvement in Classification Results

This section compares different augmentation approaches in terms of the overall accuracy and Kappa statistics of the corresponding classification results. Experiments reveal that the classification frameworks adopted in this article overfit 400 samples. Table VI presents the results of the comparisons where 70% of the total 900 samples are augmented training samples, i.e., 630 augmented and 270 actual samples. In the graphs presented in Fig. 4, different augmentation approaches are compared for varying percentages of actual training samples where 650 training samples are employed. Note that when the percentage of actual training samples is less than 60%, the DL-based augmentations do not give acceptable results. As is evident from the

TABLE IV
COMPARISON OF THE DEVIATION OF THE TREND OF THE AUGMENTED VI CURVE SAMPLES FROM THE TREND OF THE AVAILABLE TRAINING SAMPLES

| Crops | Data Augmentation Technique | Cosine similarity with the trend |
|---|---|---|
| Wheat | Fourier based [54] | 0.949 |
| | Wavelet transform-based [53] | 0.975 |
| | The proposed approach without modelling the trends and phenological events as discussed in section 2A | 0.986 |
| | DL based [18] | 0.969 |
| | Proposed approach | 0.998 |
| Barley | Fourier based [54] | 0.945 |
| | Wavelet transform-based [53] | 0.953 |
| | The proposed approach without modelling the trends and phenological events as discussed in section 2A | 0.979 |
| | DL based [18] | 0.958 |
| | Proposed approach | 0.996 |

TABLE V
COMPARISON OF COMPUTATIONAL PERFORMANCE OF AUGMENTATION TECHNIQUES

| Crops | Data Augmentation Technique | Time (s) |
|---|---|---|
| Wheat | Fourier based [54] | 213 |
| | Wavelet transform-based [53] | 134 |
| | DL based [18] | 489 |
| | Proposed approach | 76 |
| Barley | Fourier based [54] | 260 |
| | Wavelet transform-based [53] | 231 |
| | DL based [18] | 619 |
| | Proposed approach | 118 |

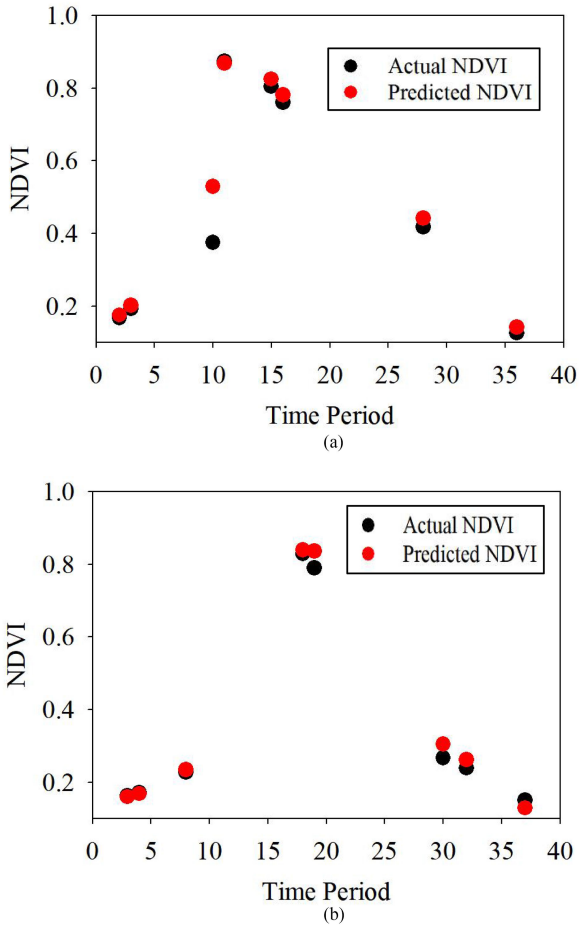


Fig. 3. Actual and predicted NDVI during crop-specific phenological events for (a) wheat and (b) barley.

results, even when the percentage of actual training samples is relatively low, the proposed augmentation approaches give good results compared to the conventional ones. In order to further illustrate the better performance of the proposed approach, a comparison of the visual results of classification is presented in Fig. 5. As is evident the proposed approach gives better results as compared to the existing state-of-the-art.

## IV. DISCUSSION

The DL-based augmentation techniques require a large number of training samples [19], [34]. DL-based approaches do not give acceptable results because this article focuses on data augmentation with minimal training samples [36]. Additionally, it is not easy to model the phenological events using DL-based approaches [40]. The classical augmentation approaches, such as translation, rotation, scaling, and wrapping, also do not preserve the characteristic phenological events of the VI curves [36], [46], [51]. Therefore, only transform-based approaches that consider the characteristic features of the index curves are suitable for the augmentation of the VI curves. Although MODWT-based augmentation approaches report good results for time series data, the non-consideration of crop-specific features makes the approach unsuitable for VI curve augmentation [7], [63].

TABLE VI
COMPARISON OF THE CLASSIFICATION RESULTS USING 270 ACTUAL TRAINING SAMPLES (AMOUNTING TO 30%) AND 630 AUGMENTED SAMPLES (AMOUNTING TO 70%)

| Classifier | Data Augmentation Technique | Overall Accuracy | Kappa statistics |
|---|---|---|---|
| GAN | Fourier based [54] | 0.55 | 61.09 |
| | Wavelet transform based [53] | 0.60 | 66.34 |
| | The proposed approach without modelling the trends and phenological events as discussed in section 2A | 0.68 | 70.09 |
| | DL based [18] | 0.60 | 64.50 |
| | Proposed approach | 0.82 | 86.97 |
| LSTM | Fourier based [54] | 0.59 | 64.84 |
| | Wavelet transform based [53] | 0.63 | 67.86 |
| | The proposed approach without modelling the trends and phenological events as discussed in section 2A | 0.65 | 71.23 |
| | DL based [18] | 0.61 | 66.50 |
| | Proposed approach | 0.84 | 88.57 |

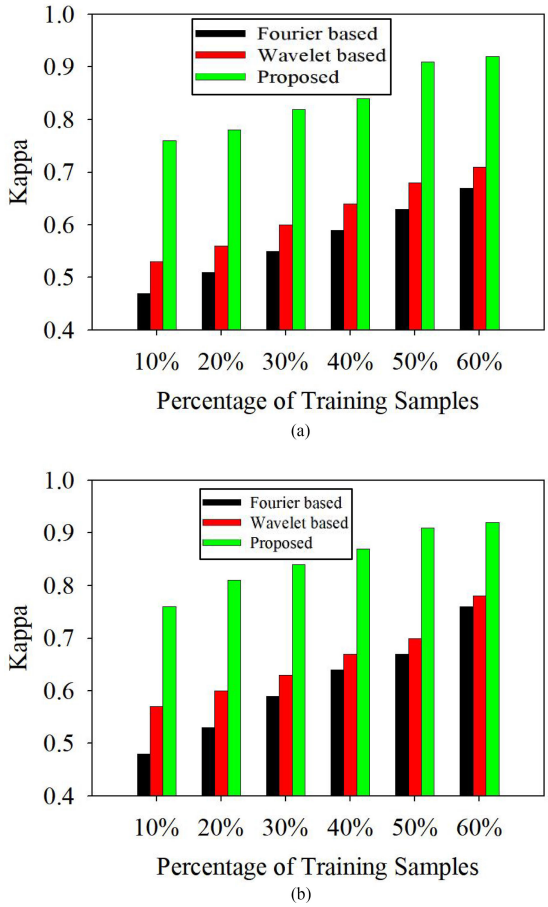


Fig. 4. Comparison of the augmentation methods for varying percentage of training samples. (a) LSTM-based classification. (b) GAN based classification.

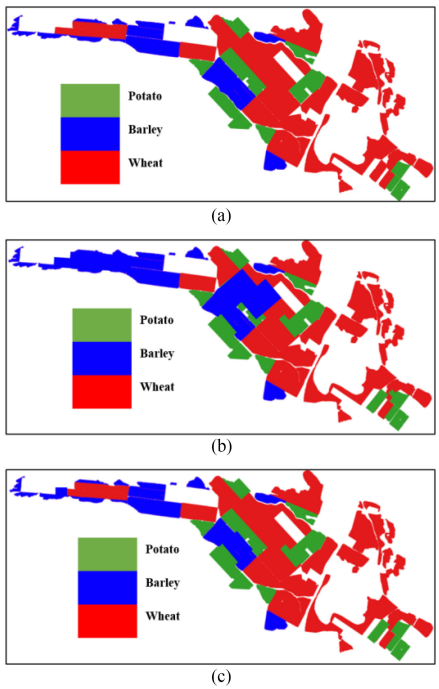


Fig. 5. Visual illustration of the proposed augmentation strategy. (a) Ground truth data. (b) Wavelet based approach. (c) Proposed augmentation strategy.

The proposed augmentation strategy of combining MODWT with entropy-based subsequence estimation generates surrogates that retain the crop-specific features and periodicities. Furthermore, phenological events and the underlying trend of the VI curves of each of the crop classes are accurately modeled using computationally optimal transformations [64]. Unlike the existing transform-based approaches, the proposed approach does not alter the wavelet coefficients that characterize a given crop class [35], [45].

This article also illustrates that the accuracy of VI curve augmentation can be estimated by comparing crop-specific phenological events, such as planting, heading, and harvesting events, of the surrogates with those of the available actual training samples. The proposed strategy of using the prior information derived from trend and seasonality to refine the transform coefficients accurately preserves the cop-specific features [54], [59]. Unlike the existing approaches that require a lot of actual training samples, the proposed approaches give good results even when actual training samples are pretty scarce [9], [65]. The generalization capability of the proposed approach can be attributed to the non-DL-based strategy of using entropy and transforms to model the characteristic features.

Although the proposed approach reduces the number of parameters and requires only a few samples, efficient finetuning of hyperparameters requires further research. In addition, alternative approaches may be adopted to identify the relevant subsequences efficiently. The generic nature of the proposed approach needs to be further investigated for different applications. The proposed approach generalizes the features based on a group of index curves belonging to a given class. The approach well preserves the crop phenological features. However, the approach is needed to be adaptive in eliminating the noisy features that may be prevalent in a group of VI curves due to environmental impacts. Although some efforts have been taken to incorporate spatial autocorrelation, an optimal strategy is needed to avoid the anomaly due to environmental impacts covering large areas.

## V. Conclusion

The massive requirement of training samples makes the data augmentation techniques essential for prominent DL-based VI curve classifiers. However, conventional augmentation approaches alter the crop-specific phenological features and are not suitable for the VI curves. Additionally, DL-based augmentation approaches are applicable only when sufficient training samples are available. This article indicates that the effective modeling of phenological characteristics is essential for the proper augmentation of the VI curves. Maximization of autocorrelation in conjunction with the variance is found to be effective in modeling crop-specific trends. The phenological events are accurately modeled as subsequences that cause entropy gain for the classification. The activation maximization is also found to be effective in identifying the most significant subsequences that are characteristics of a given crop. The proposed augmentation strategy of using MODWT, crop-specific trends, and phenological events,

to obtain the surrogates significantly improves the results. The phenological-event-based comparison of surrogates with respect to the actual training samples is found to be more effective than the confusion-matrix-based approaches for estimating the accuracy of augmentation strategies. The better performance of the proposed approach compared to the existing approaches can be attributed to the proper modeling and use of phenological events to fix the characteristic MODWT coefficients. However, the incorporation of spatial autocorrelation to the proposed augmentation strategy requires further investigation. Additionally, an optimal strategy is needed to avoid the generalization of anomalies caused by environmental impacts.

## ACKNOWLEDGMENT

The authors would like to thank Mrs. N. Panov and Mr. A. Yupiter Vanunu for the collection and processing of the datasets used in this article.

## REFERENCES

[1] J. Zhang, L. Feng, and F. Yao, "Improved maize cultivated area estimation over a large scale combining MODIS-EVI time series data and crop phenological information," *ISPRS J. Photogramm. Remote Sens.*, vol. 94, pp. 102–113, Aug. 2014, doi: 10.1016/j.isprsjprs.2014.04.023.

[2] G. Zhang *et al.*, "Mapping paddy rice planting areas through time series analysis of MODIS land surface temperature and vegetation index data," *ISPRS J. Photogramm. Remote Sens.*, vol. 106, pp. 157–171, Aug. 2015, doi: 10.1016/j.isprsjprs.2015.05.011.

[3] L. Zhong, L. Hu, L. Yu, P. Gong, and G. S. Biging, "Automated mapping of soybean and corn using phenology," *ISPRS J. Photogramm. Remote Sens.*, vol. 119, pp. 151–164, Sep. 2016, doi: 10.1016/j.isprsjprs.2016.05.014.

[4] D. P. Roy and L. Yan, "Robust Landsat-based crop time series modelling," *Remote Sens. Environ.*, vol. 238, Mar. 2020, Art. no. 110810, doi: 10.1016/j.rse.2018.06.038.

[5] Z. Yi, L. Jia, and Q. Chen, "Crop classification using multi-temporal sentinel-2 data in the Shiyang river Basin of China," *Remote Sens.*, vol. 12, no. 24, Dec. 2020, Art. no. 4052, doi: 10.3390/rs12244052.

[6] L. Zhong, L. Hu, and H. Zhou, "Deep learning based multi-temporal crop classification," *Remote Sens. Environ.*, vol. 221, pp. 430–443, Feb. 2019, doi: 10.1016/j.rse.2018.11.032.

[7] K. Zhao *et al.*, "Detecting change-point, trend, and seasonality in satellite time series data to track abrupt changes and nonlinear dynamics: A Bayesian ensemble algorithm," *Remote Sens. Environ.*, vol. 232, Oct. 2019, Art. no. 111181, doi: 10.1016/j.rse.2019.04.034.

[8] L. Zeng, B. D. Wardlow, D. Xiang, S. Hu, and D. Li, "A review of vegetation phenological metrics extraction using time-series, multispectral satellite data," *Remote Sens. Environ.*, vol. 237, Feb. 2020, Art. no. 111511, doi: 10.1016/j.rse.2019.111511.

[9] D. Al-Shammari, I. Fuentes, B. M. Whelan, P. Filippi, and T. F. A. Bishop, "Mapping of cotton fields within-season using phenology-based metrics derived from a time series of landsat imagery," *Remote Sens.*, vol. 12, no. 18, Sep. 2020, Art. no. 3038, doi: 10.3390/rs12183038.

[10] M. Xiang, Q. Yu, and W. Wu, "From multiple cropping index to multiple cropping frequency: Observing cropland use intensity at a finer scale," *Ecological Indicators*, vol. 101, pp. 892–903, Jun. 2019, doi: 10.1016/j.ecolind.2019.01.081.

[11] Y. Meng, S. N. Qasem, M. Shokri, and S. Shahab, "Dimension reduction of machine learning-based forecasting models employing principal component analysis," *Mathematics*, vol. 8, no. 8, Jul. 2020, Art. no. 1233, doi: 10.3390/math8081233.

[12] Y. Kiarashinejad, S. Abdollahramezani, and A. Adibi, "Deep learning approach based on dimensionality reduction for designing electromagnetic nanostructures," *NPJ Comput. Mater.*, vol. 6, no. 1, pp. 1–12, Dec. 2020, doi: 10.1038/s41524-020-0276-y.

[13] Y. Cheng, D. Wang, P. Zhou, and T. Zhang, "A survey of model compression and acceleration for deep neural networks," *arXiv:1710.09282 [cs.LG]*, Oct. 2017. Accessed: Oct 25, 2020. [Online]. Available: https://arxiv.org/abs/1710.09282

[14] D. Tuia, M. Volpi, L. Copa, M. Kanevski, and J. Muñoz-Marí, "A survey of active learning algorithms for supervised remote sensing image classification," *IEEE J. Sel. Topics Signal Process.*, vol. 5, no. 3, pp. 606–617, Jun. 2011, doi: 10.1109/JSTSP.2011.2139193.

[15] M. El Amin Larabi, S. Chaib, K. Bakhti, and M. S. Karoui, "Transfer learning for changes detection in optical remote sensing imagery," in *Proc. IEEE Int. Geosci. Remote Sens. Symp.*, Nov. 2019, pp. 1582–1585, doi: 10.1109/igarss.2019.8900296.

[16] H. Huang, J. Wang, C. Liu, L. Liang, C. Li, and P. Gong, "The migration of training samples towards dynamic global land cover mapping," *ISPRS J. Photogramm. Remote Sens.*, vol. 161, pp. 27–36, Mar. 2020, doi: 10.1016/j.isprsjprs.2020.01.010.

[17] J. Radoux, C. Lamarche, E. Van Bogaert, S. Bontemps, C. Brockmann, and P. Defourny, "Automated training sample extraction for global land cover mapping," *Remote Sens.*, vol. 6, no. 5, pp. 3965–3987, May 2014, doi: 10.3390/rs6053965.

[18] E. D. Cubuk, B. Zoph, J. Shlens, and Q. V. Le, "RandAugment: Practical automated data augmentation with a reduced search space," in *Proc. IEEE/CVF Conf. Comput. Vis. Pattern Recognit. Workshops*, Sep. 2019, pp. 3008–3017. Accessed: Oct. 25, 2020. [Online]. Available: http://arxiv.org/abs/1909.13719

[19] R. Anirudh, J. J. Thiagarajan, B. Kailkhura, and P. T. Bremer, "MimicGAN: Robust projection onto image manifolds with corruption mimicking," *Int. J. Comput. Vis.*, vol. 128, no. 10/11, pp. 2459–2477, Nov. 2020, doi: 10.1007/s11263-020-01310-5.

[20] X. Yang *et al.*, "A survey on smart agriculture: Development modes, technologies, and security and privacy challenges," *IEEE/CAA J. Automatica Sinica*, vol. 8, no. 2, pp. 273–302, Feb. 2021, doi: 10.1109/JAS.2020.1003536.

[21] Z. Zhang *et al.*, "A novel deep learning approach with data augmentation to classify motor imagery signals," *IEEE Access*, vol. 7, pp. 15945–15954, 2019, doi: 10.1109/ACCESS.2019.2895133.

[22] A. Makhzani, J. Shlens, N. Jaitly, I. Goodfellow, and B. Frey, "Adversarial autoencoders," Nov. 2015. Accessed: Nov. 23, 2020. [Online]. Available: http://arxiv.org/abs/1511.05644

[23] J. Gui, Z. Sun, Y. Wen, D. Tao, and J. Ye, "A review on generative adversarial networks: Algorithms, theory, and applications," *arXiv:2001.06937 [cs.LG]*, Jan. 2020. Accessed: Oct. 25, 2020. [Online]. Available: http://arxiv.org/556 abs/2001.06937

[24] L. Girin, S. Leglaive, X. Bie, J. Diard, T. Hueber, and X. Alameda-Pineda, "Dynamical variational autoencoders: A comprehensive review," Aug. 2020. Accessed: Oct. 25, 2020. [Online]. Available: http://arxiv.org/abs/2008.12595

[25] Y. Hoshen, "Non-adversarial mapping with VAES," in *Proc. Adv. Neural Inf. Process. Syst.*, 2018, pp. 7528–7537.

[26] I. J. Goodfellow *et al.*, "Generative adversarial nets," in *Proc. Adv. Neural Inf. Process. Syst.*, 2014, vol. 3, pp. 2672–2680, doi: 10.3156/jsoft.29.5_177_2.

[27] M. Mirza and S. Osindero, "Conditional generative adversarial nets," Nov. 2014. Accessed: Apr. 2, 2021. [Online]. Available: http://arxiv.org/abs/1411.1784

[28] T. Miyato, T. Kataoka, M. Koyama, and Y. Yoshida, "Spectral normalization for generative adversarial networks," Feb. 2018. Accessed: Apr. 2, 2021. [Online]. Available: https://github.com/pfnet-research/sngan_

[29] M. Buda, A. Maki, and M. A. Mazurowski, "A systematic study of the class imbalance problem in convolutional neural networks," *Neural Netw.*, vol. 106, pp. 249–259, Oct. 2017, doi: 10.1016/j.neunet.2018.07.011.

[30] A. Odena, C. Olah, and J. Shlens, "Conditional image synthesis with auxiliary classifier gans," in *Proc. 34th Int. Conf. Mach. Learn.*, Jul. 2017, vol. 6, pp. 4043–4055. Accessed: Apr. 2, 2021. [Online]. Available: https://github.com/openai/improved-gan/

[31] A. Ali-Gombe, E. Elyan, Y. Savoye, and C. Jayne, "Few-shot classifier GAN," in *Proc. Int. Joint Conf. Neural Networks (IJCNN)*, Oct. 2018, pp. 1–8, doi: 10.1109/IJCNN.2018.8489387.

[32] C. Huang, Y. Li, C. C. Loy, and X. Tang, "Deep imbalanced learning for face recognition and attribute prediction," *IEEE Trans. Pattern Anal. Mach. Intell.*, vol. 42, no. 11, pp. 2781–2794, Nov. 2020, doi: 10.1109/TPAMI.2019.2914680.

[33] G. Mariani, F. Scheidegger, R. Istrate, C. Bekas, and C. Malossi, "BAGAN: Data augmentation with balancing GAN," Mar. 2018. Accessed: Apr. 3, 2021. [Online]. Available: http://arxiv.org/abs/1803.09655

[34] A. Ali-Gombe, E. Elyan, and C. Jayne, "Multiple fake classes GAN for data augmentation in face image dataset," in *Int. Joint Conf. Neural Networks (IJCNN)*, Jul. 2019, pp. 1–8, doi: 10.1109/IJCNN.2019.8851953.

[35] Q. Wen, L. Sun, X. Song, J. Gao, X. Wang, and H. Xu, "Time series data augmentation for deep learning: A survey," Feb. 2020. Accessed: Apr. 1, 2021. [Online]. Available: http://arxiv.org/abs/2002.12478
[36] B. K. Iwana and S. Uchida, "An empirical survey of data augmentation for time series classification with neural networks," Jul. 2020. Accessed: Apr. 3, 2021. [Online]. Available: http://arxiv.org/abs/2007.15951
[37] L. Zhang, "Transfer adaptation learning: A decade survey," *arXiv:1903.04687 [cs.CV]*, Mar. 2019. Accessed: Oct. 25, 2020. [Online]. Available: https://arxiv.org/abs/1903.04687
[38] C. Oh, S. Han, and J. Jeong, "Time-Series data augmentation based on interpolation," *Procedia Comput. Sci.*, vol. 175, pp. 64–71, Jan. 2020, doi: 10.1016/J.PROCS.2020.07.012.
[39] Q. Wen *et al.*, "Time series data augmentation for deep learning: A survey," in *Proc. 30th Int. Joint Conf. Artif. Intell.*, Feb. 2021, pp. 4653–4660, doi: 10.24963/ijcai.2021/631.
[40] S. C. Wong, A. Gatt, V. Stamatescu, and M. D. McDonnell, "Understanding data augmentation for classification: When to warp?," in *Proc. Int. Conf. Digit. Image Comput., Techn. Appl.*, 2016, pp. 1–6, doi: 10.1109/DICTA.2016.7797091.
[41] W. Wang, X. Liu, and X. Mou, "Data augmentation and spectral structure features for limited samples hyperspectral classification," *Remote Sens.*, vol. 13, no. 4, pp. 1–23, Feb. 2021, doi: 10.3390/rs13040547.
[42] C. Shorten and T. M. Khoshgoftaar, "A survey on image data augmentation for deep learning," *J. Big Data*, vol. 6, no. 1, Dec. 2019, Art. no. 60, doi: 10.1186/s40537-019-0197-0.
[43] R. Simoes *et al.*, "Land use and cover maps for mato grosso state in Brazil from 2001 to 2017," *Sci. Data*, vol. 7, no. 1, pp. 1–10, Dec. 2020, doi: 10.1038/s41597-020-0371-4.
[44] L. Malambo and C. D. Heatwole, "Automated training sample definition for seasonal burned area mapping," *ISPRS J. Photogramm. Remote Sens.*, vol. 160, pp. 107–123, Feb. 2020, doi: 10.1016/j.isprsjprs.2019.11.026.
[45] T. Fields, G. Hsieh, and J. Chenou, "Mitigating drift in time series data with noise augmentation," in *Proc. 6th Annu. Conf. Comput. Sci. Comput. Intell.*, Dec. 2019, pp. 227–230, doi: 10.1109/CSCI49370.2019.00046.
[46] A. Le Guennec, S. Malinowski, and R. Tavenard, "Data augmentation for time series classification using convolutional neural networks," in *Proc. ECML/PKDD Work. Adv. Anal. Learn. Temporal Data*, 2016, Accessed: Apr. 3, 2021. [Online]. Available: https://halshs.archives-ouvertes.fr/halshs-01357973
[47] T. T. Um *et al.*, "Data augmentation of wearable sensor data for parkinson's disease monitoring using convolutional neural networks," in *Proc. 19th ACM Int. Conf. Multimodal Interact.*, 2017, pp. 216–220, doi: 10.1145/3136755.3136817.
[48] N. Jaitly and G. E. Hinton, "Vocal tract length perturbation (VTLP) improves speech recognition," in *Proc. 30th Int. Conf. Mach. Learn.*, vol. 90, pp. 42–51, 2013. Accessed: Apr. 3, 2021. [Online]. Available: http://www.iarpa.gov/
[49] V. Maus, G. CÄmara, R. Cartaxo, A. Sanchez, F. M. Ramos, and G. R. De Queiroz, "A time-weighted dynamic time warping method for land-use and land-cover mapping," *IEEE J. Sel. Topics Appl. Earth Obs. Remote Sens.*, vol. 9, no. 8, pp. 3729–3739, Aug. 2016, doi: 10.1109/JSTARS.2016.2517118.
[50] J. Fowler, F. Waldner, and Z. Hochman, "All pixels are useful, but some are more useful: Efficient in situ data collection for crop-type mapping using sequential exploration methods," *Int. J. Appl. Earth Observ. Geoinformat.*, vol. 91, Sep. 2020, Art. no. 102114, doi: 10.1016/j.jag.2020.102114.
[51] M. Belgiu, W. Bijker, O. Csillik, and A. Stein, "Phenology-based sample generation for supervised crop type classification," *Int. J. Appl. Earth Obs. Geoinformat.*, vol. 95, Mar. 2021, Art. no. 102264, doi: 10.1016/j.jag.2020.102264.
[52] C. J. Keylock, "A wavelet-based method for surrogate data generation," *Physica D Nonlinear Phenomena*, vol. 225, no. 2, pp. 219–228, Jan. 2007, doi: 10.1016/j.physd.2006.10.012.
[53] G. Lancaster, D. Iatsenko, A. Pidde, V. Ticcinelli, and A. Stefanovska, "Surrogate data for hypothesis testing of physical systems," *Phys. Rep.*, vol. 748, pp. 1–60, Jul. 2018, doi: 10.1016/j.physrep.2018.06.001.
[54] J. H. Lucio, R. Valdés, and L. R. Rodríguez, "Improvements to surrogate data methods for nonstationary time series," *Phys. Rev. E - Statist. Nonlinear Soft Matter Phys.*, vol. 85, no. 5, May 2012, Art. no. 056202, doi: 10.1103/PhysRevE.85.056202.
[55] L. Vergara, A. Salazar, J. Belda, G. Safont, S. Moral, and S. Iglesias, "Signal processing on graphs for improving automatic credit card fraud detection," in *Proc. -Int. Carnahan Conf. Secur. Technol.*, Dec. 2017, pp. 1–6, doi: 10.1109/CCST.2017.8167820.
[56] S. Kayal, F. Dubost, H. A. W. M. Tiddens, and M. De Bruijne, "Spectral data augmentation techniques to quantify lung pathology from CT-Images," in *Proc. Int. Symp. Biomed. Imag.*, Apr. 2020, pp. 586–590, doi: 10.1109/ISBI45749.2020.9098581.
[57] Q. Wen, J. Gao, X. Song, L. Sun, H. Xu, and S. Zhu, "RobustSTL: A robust seasonal-trend decomposition algorithm for long time series," in *Proc. 33rd AAAI Conf. Artif. Intell. AAAI, 31st Innov. Appl. Artif. Intell. Conf. IAAI, 9th AAAI Symp. Educ. Adv. Artif. Intell. EAAI*, 2019, pp. 5409–5416. Accessed: Jun. 7, 2021. [Online]. Available: http://arxiv.org/abs/1812.01767
[58] J. Gao, X. Song, Q. Wen, P. Wang, L. Sun, and H. Xu, "RobustTAD: Robust time series anomaly detection via decomposition and convolutional neural networks," Feb. 2020. Accessed: Jun. 16, 2021. [Online]. Available: http://arxiv.org/abs/2002.09545
[59] M. A. Haugen, B. Rajaratnam, and P. Switzer, "Extracting common time trends from concurrent time series: Maximum autocorrelation factors with application to tree ring time series data," Feb. 2015. Accessed: Jun. 8, 2021. [Online]. Available: http://arxiv.org/abs/1502.01073
[60] J. Grabocka, N. Schilling, M. Wistuba, and L. Schmidt-Thieme, "Learning time-series shapelets," in *Proc. ACM SIGKDD Int. Conf. Knowl. Discov. Data Mining*, 2014, pp. 392–401, doi: 10.1145/2623330.2623613.
[61] L. Zhu, Y. Wang, and Q. Fan, "MODWT-ARMA model for time series prediction," *Appl. Math. Model.*, vol. 38, no. 5/6, pp. 1859–1865, Mar. 2014, doi: 10.1016/j.apm.2013.10.002.
[62] T. D. Pham, "Time–frequency time–space LSTM for robust classification of physiological signals," *Sci. Rep.*, vol. 11, no. 1, pp. 1–11, Dec. 2021, doi: 10.1038/s41598-021-86432-7.
[63] X. You, J. Meng, M. Zhang, and T. Dong, "Remote sensing based detection of crop phenology for agricultural zones in China using a new threshold method," *Remote Sens.*, vol. 5, no. 7, pp. 3190–3211, Jul. 2013, doi: 10.3390/rs5073190.
[64] L. Feng, Y. Wang, Z. Zhang, and Q. Du, "Geographically and temporally weighted neural network for winter wheat yield prediction," *Remote Sens. Environ.*, vol. 262, Sep. 2021, Art. no. 112514, doi: 10.1016/J.RSE.2021.112514.
[65] J. Li, Y. Shen, and C. Yang, "An adversarial generative network for crop classification from remote sensing timeseries images," *Remote Sens.*, vol. 13, no. 1, pp. 1–15, Dec. 2021, doi: 10.3390/rs13010065.

**P. V. Arun** (Student Member, IEEE) received the Ph.D. degree in novel deep learning algorithms for hyperspectral image processing from the Indian Institute of Technology, Bombay, Mumbai, India, in 2020.

He is currently an Assistant Professor with the Indian Institute of Information Technology, Sri City with expertise in modeling and designing deep learning algorithms for analysis of multimodal remote sensing datasets. He completed his Postdoctoral Research with the Remote Sensing Lab, Ben-Gurion University of the Negev. He has authored and coauthored more than 14 international journal and around ten international conference publications.

Dr. Arun was a Reviewer of several reputed international journals.

**Arnon Karnieli** (Member, IEEE) received the Ph.D. degree from the University of Arizona, Tucson, AZ, USA, in 1988.

He is currently the Head of the Remote Sensing Laboratory, Jacob Blaustein Institutes for Desert Research, Ben-Gurion University of the Negev, Sede Boker Campus, Israel. He supervised tens of master students, 15 Ph.D. students, and several Postdocs. His study applications cover dryland ecosystems and agriculture, and to a lesser extent dust/aerosols and coastal water. He has authored or coauthored more than 240 papers in peer-reviewed journals. His H index = 45 (ISI). His main research interests include the processing of spaceborne, airborne, and ground spectroscopic data of drylands concerning desertification and climate change processes.

Dr. Karnieli was ranked among the top 20 researchers in the world in the field of remote sensing discipline by *Scientometricsc* journal in 2013. In 2020, he was ranked by PLOS Biology among the top 2% scientists worldwide. He is the Israeli Principal Investigator of the recreantly launched Vegetation and Environmental NewMicro Spacecraft (VEN$\mu$S) mission.